Synthesis of Ordered and Disordered Silicas with Uniform Pores on the Border between Micropore and Mesopore Regions Using Short Double-Chain Surfactants

Ryong Ryoo,*,† In-Soo Park,† Shinae Jun,† Chul Wee Lee,‡ Michal Kruk,§ and Mietek Jaroniec*,§

Contribution from the Department of Chemistry, School of Molecular Science-BK21, Korea Advanced Institute of Science and Technology, Taejon 305-701, Korea, Industrial Catalysis Research Laboratory, Korea Research Institute of Chemical Technology, Taejon 305-606, Korea, and Department of Chemistry, Kent State University, Kent, Ohio 44242

Received October 31, 2000

Abstract: Silica molecular sieves with uniform pores on the borderline between micropore (diameter <2 nm) and mesopore (from 2 to 50 nm) ranges were synthesized by a novel method using judiciously chosen mixtures of short double-chain alkylammonium surfactants. These silicas were characterized using X-ray diffraction (XRD), thermogravimetry, and nitrogen and argon adsorption. The calcined materials exhibited either 2-dimensional (2-D) hexagonal or disordered structures with XRD interplanar spacing from 2.51 to 2.93 nm, including the value of as small as 2.69 nm for highly ordered 2-D hexagonal silica. The dependence of the pore size and surfactant content on the surfactant chain length provided strong evidence for supramolecular templating being operative in the formation of small-pore silicas, even for the surfactant chain length of six carbon atoms. Both hexagonally ordered and disordered calcined samples were shown to exhibit narrow pore size distributions with maxima in the range from 1.96 to 2.61 nm (reliably evaluated on the basis of the unit-cell dimension and pore volume for 2-D hexagonal materials, and calculated using a properly calibrated procedure), tailored by the surfactant chain length. The samples exhibited primary pore volumes from 0.28 to 0.54 $cm^3\ g^{-1}$ and specific surface areas from 730 to 930 $m^2\ g^{-1}$. Because of their small yet uniform pore size and large specific surface area, the silicas reported herein promise to be useful in applications in adsorption and catalysis. Adsorption studies of these materials provided a unique new insight into the pore-filling mechanism for small-pore materials. Moreover, the approach proposed herein is expected to facilitate the synthesis of not only small-pore silicas but also materials with other framework compositions, thus largely contributing to bridging the gap in attainable pore sizes between micropore and mesopore ranges.

Introduction

The recent discovery of synthesis routes using surfactants as structure-directing agents remarkably extended the range of pore sizes attainable for periodic porous materials, from conventional zeolite pores (diameter <1.3 nm) to those of ordered mesoporous materials (from 2.7 to 12 nm).[1−6] The initially reported studies[1] of silicas with 2-dimensional (2-D) hexagonally ordered arrays of approximately cylindrical pores (herein referred to as MCM-41-type materials) claimed that the materials with diameters from 1.6 to 10 nm could be obtained using alkyltrimethylammonium surfactant templates of different alkyl chain lengths, without or with the addition of a proper amount of micelle expanders.[1] Numerous following works confirmed that highly ordered MCM-41-type silicas with (100) interplanar spacings, d_{100}, from ∼3 to 7 nm and pore sizes from ∼2.7 to at least 6.5 nm can be synthesized using the alkylammonium surfactants of chain lengths from 10 to 22 carbon atoms.[7−12] The synthesis of materials with ordered pores of diameters corresponding to those between the upper limit for zeolites and the lower end of the aforementioned mesopore size range (that is, between 1.3 and 2.7 nm) is of particular interest because of its great scientific and utilitarian importance.[13−15] However, the

* Correspondence should be addressed to Prof. R. Ryoo (E-mail: rryoo@sorak.kaist.ac.kr) for synthesis and Prof. M. Jaroniec (E-mail: jaroniec@columbo.kent.edu) for characterization.

† Korea Advanced Institute of Science and Technology.

‡ Korea Research Institute of Chemical Technology.

§ Kent State University.

(1) Beck, J. S.; Vartuli, J. C.; Roth, W. J.; Leonowicz, M. E.; Kresge, C. T.; Schmitt, K. D.; Chu, C. T.-W.; Olson, D. H.; Sheppard, E. W.; McCullen, S. B.; Higgins, J. B.; Schlenker, J. L. *J. Am. Chem. Soc.* **1992**, *114*, 10834−10843.

(2) Yanagisawa, T.; Shimizu, T.; Kuroda, K.; Kato, C. *Bull. Chem. Soc. Jpn.* **1990**, *63*, 988−992.

(3) Inagaki, S.; Fukushima, Y.; Kuroda, K. *J. Chem. Soc., Chem. Commun.* **1993**, 680−682.

(4) Bagshaw, S. A.; Prouzet, E.; Pinnavaia, T. J. *Science* **1995**, *269*, 1242−1244.

(5) Zhao, D.; Huo, Q.; Feng, J.; Chmelka, B. F.; Stucky, G. D. *J. Am. Chem. Soc.* **1998**, *120*, 6024−6036.

(6) Lettow, J. S.; Han, Y. J.; Schmidt-Winkel, P.; Yang, P.; Zhao, D.; Stucky, G. D.; Ying, J. Y. *Langmuir* **2000**, *16*, 8291−8295.

(7) Huo, Q.; Margolese, D. I.; Stucky, G. D. *Chem. Mater.* **1996**, *8*, 1147−1160.

(8) Khushalani, D.; Kuperman, A.; Ozin, G. A.; Tanaka, K.; Garces, J.; Olken, M. M.; Coombs, N. *Adv. Mater.* **1995**, *7*, 842−846.

(9) Cheng, C.-F.; Zhou, W.; Park, D. H.; Klinowski, J.; Hargreaves, M.; Gladden, L. F. *J. Chem. Soc., Faraday Trans.* **1997**, *93*, 359−363.

(10) Corma, A.; Kan, Q.; Navarro, M. T.; Perez-Pariente, J.; Rey, F. *Chem. Mater.* **1997**, *9*, 2123−2126.

(11) Kruk, M.; Jaroniec, M.; Sakamoto, Y.; Terasaki, O.; Ryoo, R.; Ko, C. H. *J. Phys. Chem. B* **2000**, *104*, 292−301.

(12) Sayari, A.; Yang, Y. *J. Phys. Chem. B* **2000**, *104*, 4835−4835.

(13) Sayari, A. *Chem. Mater.* **1996**, *8*, 1840−1852.

(14) Corma, A. *Chem. Rev.* **1997**, *97*, 2373−2419.

10.1021/ja0038326 CCC: $20.00
Published on Web 02/02/2001

attempts to further decrease the unit-cell size and pore size of MCM-41-type silicas synthesized using octyltrimethylammonium surfactant afforded poorly ordered materials,[16−21] and hexyltrimethylammonium surfactant was found to be unsuitable as a supramolecular template.[16] In contrast, short-chain neutral alkylamines and diaminealkyls were found to be suitable as supramolecular templates for the synthesis of hexagonally ordered or disordered niobium oxide with very small unit-cell dimension and pore size within the micropore range.[22,23] Unfortunately, the extension of this templating procedure unto porous silicas was only partially successful,[24] because it afforded silicas of the desired small interplanar spacing of ∼2.5 nm and pore size <2 nm, but the materials had a tendency to collapse upon storage. It was also observed that the calcined materials might contain a mesostructured impurity phase.

In some cases, it was possible to obtain MCM-41-type silicas with small unit-cell dimensions using common alkylammonium templates, such as cetyltrimethylammonium ($CTMA^+$),[25−28] due to the exceptionally large degree of shrinkage upon surfactant removal via calcination.[25−27] In this way, ordered films with d_{100} as small as 2.2−2.8 nm were prepared.[25,26] From the reported data,[26] it is clear that at least one of these samples (prepared via calcination of material obtained from co-condensation of tetraethyl orthosilicate and vinyltriethoxysilane) had accessible primary pores of size exclusively <2 nm. However, the details of the porous structure of these materials as well as the reproducibility of the pore size and the suitability of this synthesis approach for silicas in other forms, such as powders, are yet to be explored. Non-silica ordered mesoporous materials with relatively small unit-cell sizes and pore diameters have also been obtained using $CTMA^+$ because of the large shrinkage that accompanied the surfactant removal via calcination.[29−31] In addition, the unit-cell shrinkage can be induced by heating at temperatures well above those necessary for the surfactant removal and facile framework condensation. This approach was used to synthesize hexagonally ordered silicas with d_{100} down to ∼3 nm.[32] However, the quality of the resulting materials was at best comparable to that of the samples prepared using alkyltrimethylammonium templates.[12,18−21]

The results discussed above point to the need for exploring new methods for the synthesis of ordered silicas having pore sizes on the borderline between the micropore and mesopore ranges. The successful synthesis of ordered non-silica materials using judiciously chosen short-chain templates[22,23,33] suggests that this methodology may also afford highly ordered small-pore supramolecular-templated silicas. To this end, the synthesis of SBA-1 silica of cubic ordered pore structure, which is capable of providing materials with relatively small pore size, perhaps close to the micropore range has been reported.[34] In this case, alkyltriethylammonium surfactants of different chain lengths were used. Likewise, the use of ω-hydroxyalkylammonium bolaform surfactants afforded ordered silicas with relatively small pore sizes,[35] although the reported adsorption data did not provide any evidence that the pore diameters of these materials were smaller, and pore structure uniformity was better than those for the alkyltrimethylammonium-templated silicas.[12,17−19,21] As recently demonstrated, templating with large single molecules[36] and collective templating with small rigid molecules[37] are also promising for the synthesis of ordered materials having pore sizes of ∼1.3−2 nm, but further studies will be needed to elucidate the details of pore structures of these interesting materials.

In this work, we demonstrate that the application of mixtures of judiciously chosen short double-chain amphiphilic surfactants resulted in significant improvement of the long-range ordering of silicas having small unit-cell sizes and made it possible to synthesize materials which exhibit X-ray diffraction (XRD) reflections, even in the case of surfactant templates with extremely short alkyl chains. In particular, materials with uniform pore sizes were obtained using the short double-chain surfactants with hexyl, heptyl, octyl and decyl chains, including highly ordered MCM-41-type samples with XRD d_{100} as small as 2.69 nm synthesized using surfactants with octyl chains. The details of a novel synthesis strategy using the short double-tail surfactants are unveiled, and the results of detained characterization of these important materials using XRD, thermogravimetry, nitrogen adsorption, and argon adsorption are reported.

Materials and Methods

Materials. The double-chain surfactants used in the synthesis were *N*,*N*′-dialkyl-*N*,*N*,*N*′,*N*′-tetramethylpropane-1,3-diammonium bromides [$C_nH_{2n+1}(CH_3)_2N(CH_2)_3N(CH_3)_2C_nH_{2n+1}Br_2$; C_{n-3-n} surfactants in short] and *N*,*N*-dialkyl-*N*,*N*-dimethylammonium bromides [$(C_nH_{2n+1})_2(CH_3)_2NBr$, C_{n-n} surfactants in short]. The C_{n-3-n} surfactants were synthesized by reaction between *N*,*N*,*N*′,*N*′-tetramethyl-1,3-diaminopropane [$(CH_3)_2N(CH_2)_3N(CH_3)_2$, 98%, TCI] and 1-bromoalkanes ($C_nH_{2n+1}Br$, Aldrich) in acetonitrile solvent under reflux at 353 K for 12 h. After the reaction, the solvent was removed using a rotary evaporator. The products were recrystallized using a chloroform−ethylacetate mixture. The C_{10-10} and C_{8-8} surfactants were synthesized by reaction between *N*,*N*-dimethyl-*n*-alkylamine [$C_nH_{2n+1}(CH_3)_2N$ 95%, TCI] and 1-bromoalkane ($C_nH_{2n+1}Br$, Aldrich) in acetonitrile solvent at 353 K for 12 h under reflux. After the reaction, the acetonitrile solvent was removed using a rotary evaporator. The 1-bromoalkane in excess was extracted with a hexane−water−ethanol system in a separatory funnel. The product contained in the water−ethanol layer was then extracted into chloroform to remove water-soluble impurities. The C_{7-7} and C_{6-6} surfactants were synthesized by a reaction between dimethylamine [$(CH_3)_2NH$, 2.0 M solution in tetrahydrofuran, Aldrich], sodium hydroxide (NaOH, Aldrich), and

(15) Ying, J. Y.; Mehnert, C. P.; Wong, M. S. *Angew. Chem., Int. Ed.* **1999**, *38*, 56−77.
(16) Beck, J. S.; Vartuli, J. C.; Kennedy, G. J.; Kresge, C. T.; Roth, W. J.; Schramm, S. E. *Chem. Mater.* **1994**, *6*, 1816−1821.
(17) Tanev, P. T.; Pinnavaia, T. J. *Chem. Mater.* **1996**, *8*, 2068−2079.
(18) Kruk, M.; Jaroniec, M.; Sayari, A. *J. Phys. Chem. B* **1997**, *101*, 583−589.
(19) Ravikovitch, P. I.; Wei, D.; Chueh, W. T.; Haller, G. L.; Neimark, A. V. *J. Phys. Chem. B* **1997**, *101*, 3671−3679.
(20) Sonwane, C. G.; Bhatia, S. K.; Calos, N. *Ind. Eng. Chem. Res.* **1998**, *37*, 2271−2283.
(21) Sonwane, C. G.; Bhatia, S. K. *Chem. Eng. Sci.* **1998**, *53*, 3143−3156.
(22) Sun, T.; Ying, J. Y. *Nature* **1997**, *389*, 704−706.
(23) Sun, T.; Ying, J. Y. *Angew. Chem., Int. Ed. Engl.* **1998**, *37*, 664−667.
(24) Eswaramoorthy, M.; Neeraj, S.; Rao, C. N. R. *Microporous Mesoporous Mater.* **1999**, *28*, 205−210.
(25) Ogawa, M. *Chem. Commun.* **1996**, 1149−1050.
(26) Ogawa, M.; Kikuchi, T. *Adv. Mater.* **1998**, *10*, 1077−1080.
(27) Aguado, J.; Serrano, D. P.; Escola, J. M. *Microporous Mesoporous Mater.* **2000**, *34*, 43−54.
(28) Serrano, D. P.; Aguado, J.; Escola, J. M.; Garagorri, E. *Chem. Commun.* **2000**, 2041−2042.
(29) Kimura, T.; Sugahara, Y.; Kuroda, K. *Chem. Commun.* **1998**, 559−560.
(30) Blanchard, J.; Schuth, F.; Trens, P.; Hudson, M. *Microporous Mesoporous Mater.* **2000**, *39*, 163−170.
(31) Chen, H. R.; Shi, J.-L.; Yu, J.; Wang, L.-Z.; Yan, D.-S. *Microporous Mesoporous Mater.* **2000**, *39*, 171−176.
(32) Naono, H.; Hakuman, M.; Shiono, T. *J. Colloid Interface Sci.* **1997**, *186*, 360−368.
(33) Antonelli, D. M. *Adv. Mater.* **1999**, *11*, 487−492.
(34) Kim, M. J.; Ryoo, R. *Chem. Mater.* **1999**, *11*, 487−491.
(35) Bagshaw, S. A.; Hayman, A. R. *Chem. Commun.* **2000**, 533−534.
(36) Larsen, G.; Lotero, E.; Marquez, M. *Chem. Mater.* **2000**, *12*, 1513−1515.
(37) Sun, T.; Wong, M. S.; Ying, J. Y. *Chem. Commun.* **2000**, 2057−2058.

Table 1. Molar Composition of Synthesis Reaction Mixtures

product	SiO_2	Na_2O	C_{n-3-n}	C_{n-n}	H_2O
C6-D	4	1	0	1	1000
C7-D	4	1	0.5	0.5	1000
C8-H	6	1.5	0.75	0.25	1500
C8-D	6	1.5	1	0	1500
C10-H	6	1.5	1	0	700

1-bromoalkane in an autoclave, equipped with a mechanical stirrer, at 338 K for 12 h. The purification of these surfactants was performed in a manner similar to the cases of C_{10-10} and C_{8-8}, except that NaBr was filtered after the reaction. The syntheses of the C_{n-3-n} and C_{n-n} surfactants were confirmed by ^{1}H NMR spectroscopy.

Disordered or hexagonally ordered silica samples were synthesized using the C_{n-3-n} and C_{n-n} surfactants as templates. The samples will be denoted as C*n*-D or C*n*-H, depending on the number of carbon atoms (*n*) in the alkyl chain of the surfactant used, and on the structure type as inferred from XRD patterns: disordered (D) for materials with a single well-pronounced XRD peak, or 2-D hexagonally ordered (H) for materials with three XRD peaks that can be indexed as (100), (110) and (200) reflections of a 2-D hexagonal structure. Synthesis of the samples was performed using the starting compositions given in Table 1. To obtain the starting compositions, an aqueous solution of the C_{n-3-n} or C_{n-n} surfactants was added to 9 wt % aqueous solution of sodium silicate (Na/Si = 0.5)[38] in a polypropylene bottle. The bottle was shaken vigorously for 5 min immediately following the addition. After further stirring for 1 h by a magnetic stirrer, the mixture was heated in an oven at 353 K for 1 day without being stirred. After cooling to room temperature, acetic acid corresponding to 1/3 of the molar amount of silica source was added to the mixture, drop by drop under vigorous magnetic stirring (the omission of this step would lower the yield of the product and result in a less ordered structure). The polypropylene bottle containing the mixture was heated again in an oven at 353 K for 3 days. The product was filtered after the oven temperature was increased to 373 K for 12 h. The filtered product was dried at 373 K without washing. The as-synthesized product was used for thermogravimetric investigation or calcined in air under static conditions at 823 K after washing with an HCl−ethanol mixture.[39]

Other silica samples, denoted as C_n MCM-41 (n = 6, 7, 8, and 10) were synthesized using the same silica source as for the C*n*-D and C*n*-H samples, but using alkyltrimethylammonium bromides [$C_nH_{2n+1}(CH_3)_3$NBr, C_n surfactants in short] as the structure-directing agents. These samples were obtained in order to compare the effects of the double-chain surfactants to those of the single-chain C_n surfactants. The C_n surfactants were synthesized via a reaction between trimethylamine [$(CH_3)_3$N, Aldrich] and 1-bromoalkane at 353 K for 12 h using an autoclave. The surfactants were purified as in the case of the C_{n-3-n} surfactants. The details of the C_n MCM-41 synthesis (n = 6−10) are the same as those reported earlier for C_{12}−C_{22} MCM-41 synthesis[40] except that the molar composition of the starting mixtures was changed to 2.8 SiO_2/0.7 Na_2O/1.0 C_n surfactant/400 H_2O.

Measurements. Powder XRD patterns were acquired on a Rigaku Miniflex diffractometer (30 kV, 15 mA) using Cu Kα radiation source. Weight change curves were recorded under flowing nitrogen on a TA Instruments TGA 2950 high-resolution thermogravimetric analyzer in high-resolution mode using the maximum heating rate of 5 K min^{-1}. Nitrogen and argon adsorption isotherms were measured at 77 K using a Micromeritics ASAP 2010 volumetric adsorption analyzer. Before the measurements, the samples were outgassed for 2 h at 473 K in the degas port of the adsorption analyzer.

Calculations. The nitrogen BET specific surface area[41,42] was calculated from adsorption data in the relative pressure range from 0.01 to 0.02. The total pore volume [42] was calculated from the amount adsorbed at the relative pressure of about 0.99. The primary mesopore volume, V_p, and the external surface area were evaluated using the α_s plot method.[42,43] It should be noted that in the current study, pores are classified on the basis of their size as micropores (diameter <2 nm), mesopores (diameter from 2 to 50 nm), and macropores (diameter >50 nm).[41] Furthermore, uniform pores of the samples are referred to as primary pores, whereas other mesopores and macropores (the latter of size below about 200−400 nm only, because pores of size above this limit are not detectable using nitrogen porosimetry) are referred to as secondary pores. The α_s plot calculations were performed in a standard reduced adsorption, α_s, interval from 1.3 to 1.65 (α_s is equal to the amount adsorbed at a given pressure divided by the amount adsorbed at a relative pressure of 0.4 for the reference adsorbent) using the reference nitrogen adsorption isotherm reported elsewhere.[43] The pore size distribution (PSD) was calculated from nitrogen adsorption data by employing the relation between the pore size and capillary condensation pressure determined using MCM-41 silicas,[44] and the algorithm based on the concept of Barrett, Joyner, and Halenda,[45] but without the simplifying assumptions employed by the latter authors. The nitrogen statistical film thickness curve (*t*-curve) suitable for these calculations was reported in tabular form elsewhere.[43] The primary pore size is defined as a maximum on PSD calculated as described above. In the case of hexagonally ordered C8-H and C10-H samples, the pore size was also evaluated using a relation between the primary mesopore diameter, w_d, primary mesopore volume, and XRD (100) interplanar spacing in hexagonally ordered array of uniform pores[44]

$$w_d = cd_{100}\left(\frac{\rho V_p}{1+\rho V_p}\right)^{1/2} \quad (1)$$

where ρ is the pore wall density, assumed to be equal to that of amorphous silica,[44] that is 2.2 g cm^{-3}, and c is a constant dependent on the pore geometry and equal to 1.213 for cylindrical pores. The latter pore shape was assumed herein. The statistical film thickness of nitrogen adsorbate in the pores of hexagonally ordered silicas was calculated as described in detail elsewhere.[44]

Results and Discussion

Synthesis Effects Due to Double-Chain Surfactants. As can be seen in Figures 1 and 2, XRD patterns for all of the samples synthesized using double-chain surfactants or mixtures thereof (samples C*n*-H and C*n*-D with n = 6, 7, 8 and 10) exhibited at least one peak, even for the C6-D material prepared using the structure-directing agent having a very short hexyl chain. The peak intensity and resolution for these samples were much better than those of samples prepared using common single-chain alkyltrimethylammonium surfactants. One of the samples that was synthesized using surfactants with octyl chains (C8-H) and the sample that was synthesized using a surfactant with decyl chains (C10-H) exhibited additional XRD peaks that were clearly seen, especially after calcination. XRD patterns for these samples indicated 2-D hexagonal structural ordering similar to that of MCM-41 silicas. The values of the interplanar spacing corresponding to the main XRD peak for the samples under study were in the range from 2.5 to 3 nm (see Table 2). In particular, the interplanar spacing of 2.51 nm for C7-D silica is among the smallest reported for supramolecular-templated silicas and comparable only to those of some calcined silica films[26] and silicas synthesized using hexylamine as a template.[24] However, in the latter case, there was evidence that samples calcined at 673 K or higher temperatures were contaminated by some mesostructured phase.[24] In contrast, calcination of the

(38) Ryoo, R.; Kim, J. M.*J. Chem. Soc., Chem. Commun.* **1995**, 711−712.
(39) Ryoo, R.; Jun, S.; Kim, J. M.; Kim, M. J. *Chem. Commun.* **1997**, 2225−2226.
(40) Ryoo, R.; Ko, C. H.; Park, I.-S. *Chem. Commun.* **1999**, 1413−1414.
(41) Sing, K. S. W.; Everett, D. H.; Haul, R. A. W.; Moscou, L.; Pierotti, R. A.; Rouquerol, J.; Siemieniewska, T. *Pure Appl. Chem.* **1985**, *57*, 603−619.
(42) Gregg, S. J.; Sing, K. S. W. *Adsorption, Surface Area and Porosity*; Academic Press: London, 1982.
(43) Jaroniec, M.; Kruk, M.; Olivier, J. P. *Langmuir* **1999**, *15*, 5410−5413.
(44) Kruk, M.; Jaroniec, M.; Sayari A. *Langmuir* **1997**, *13*, 6267−6273.
(45) Barrett, E. P.; Joyner, L. G.; Halenda, P. P. *J. Am. Chem. Soc.* **1951**, *73*, 373−380.

Table 2. XRD and Thermogravimetric Properties of the Samples

sample	XRD interplanar spacing[a] (uncalcined), nm	XRD interplanar spacing[a] (calcined), nm	weight loss between 373 and 623 K%	residue at 1270 K %	estimated SiO_2:N molar ratio
C6-D	2.91	2.91	21	70	11.8:1
C7-D	2.57	2.51	27	65	7.6:1
C8-H	2.79	2.69	25	64	8.0:1
C8-D	2.72	2.70	25	64	7.7:1
C10-H	3.05	2.93	28	65	7.9:1

[a] Interplanar spacing corresponds to the position of the main peak on the XRD pattern. In the case of C8-H and C10-H samples, this peak can be indexed as (100).

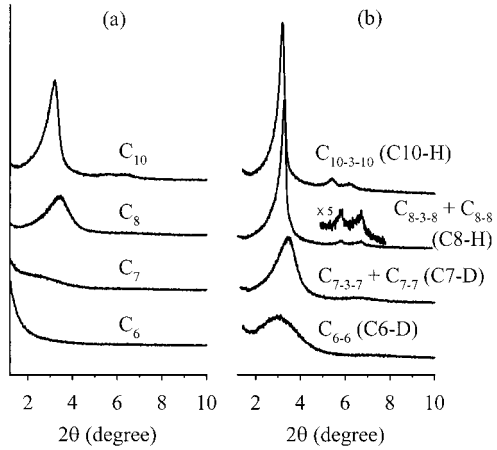

Figure 1. XRD patterns of calcined silica materials obtained following the synthesis procedure for MCM-41 using alkyltrimethylammonium bromides (a) and those synthesized using judiciously chosen surfactants (or mixtures of surfactants) with double C_6−C_{10} alkyl chains (b). These XRD patterns are similar to those of as-synthesized samples, except for an increase in intensity and decrease in the *d* spacing after calcination.

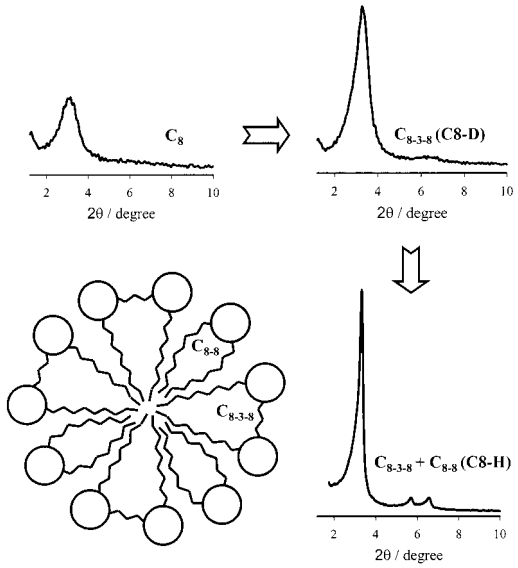

Figure 2. XRD patterns and a schematic model for the cross section of surfactant micelles, illustrating the effects of double-chain surfactants in the present synthesis. Silica sample (C8-D) synthesized with double-chain C_{8-3-8} surfactant exhibited a very intense XRD peak, as compared to samples obtained with single-chain C_8 surfactant. When synthesis was performed with the addition of C_{8-8} surfactant to the C_{8-3-8} surfactant, the resultant silica (C8-H) exhibited three narrow XRD peaks, indicating a highly ordered hexagonal structure.

samples described herein (carried out at much higher temperature) did not result in any major change in the XRD patterns but increased their relative intensity, as was expected from the improvement of the scattering contrast between the pore wall and the pore interior,[46] and led to a small decrease in the XRD interplanar spacing, thus showing that surfactant can be removed without degradation of the porous structure. C8-H is most likely the first reported example of supramolecular-templated silica with (100) interplanar spacing as low as 2.69 nm, that exhibits three clear peaks characteristic of 2-D hexagonal porous structure. The quality of the XRD pattern for C10-H silica was comparable to that for recently reported MCM-41 samples synthesized using decyltrimethylammonium surfactant[12] with the same alkyl chain length as that for the surfactant used for the preparation of C10-H. The sample templated by a surfactant with a hexyl chain had unexpectedly large XRD interplanar spacing.

As illustrated in Figure 2, two design factors were considered in the choice of the double-chain C_{n-3-n} and C_{n-n} surfactants in the present synthesis: (i) enhancement of the ability to form micelles, and (ii) optimization of surfactant packing properties. First, the increased propensity to micelle formation was expected for double-chain surfactants when compared to single-chain surfactants with the same alkyl chain length. To this end, the reported critical micelle concentration for $C_{12-3-12}$ surfactant[47] is >1 order of magnitude lower than that reported for C_{12} surfactant.[48] However, it should be noted that one needs to be cautious when predicting the supramolecular-templating ability of a given surfactant on the basis of the micelle formation behavior of pure surfactant in solution. This is because the formation of ordered surfactant-inorganic composites usually involves the formation of surfactant−inorganic ion pairs and their subsequent self-assembly and thus does not require the existence of preformed micellar templates.[49] Because of this nature of the process, surfactant−inorganic interactions may largely modify the surfactant behavior. This commonly manifests itself in the formation of surfactant−inorganic micellar structures (i) at surfactant concentrations much lower than those necessary for the formation of such micellar structures in the absence of inorganics, or (ii) under conditions otherwise unfavorable for micelle formation.[49]

The second design factor considered here was to optimize the surfactant packing properties by choosing an appropriate double-chain surfactant or, if needed, by mixing two types of double chain surfactants. The need for such optimization becomes clear on the basis of the following findings. C_n surfactants were found to favor the 2-D hexagonal phase for $n = 10-18$, whereas the lamellar phase was a typical product for $n = 20$.[7] However, the increase in the effective headgroup size using alkyltriethylammonium in addition to or instead of C_n surfactants resulted in the formation of a highly ordered 2-D

(46) Marler, B.; Oberhagemann, U.; Vortmann, S.; Gies, H. *Microporous Mater.* **1996**, *6*, 375−383.
(47) Alami, E.; Beinert, G.; Marie, P.; Zana, R. *Langmuir* **1993**, *9*, 1465−1467.
(48) Tanaka, A.; Ikeda, S. *Colloids Surf.* **1991**, *56*, 217−228.
(49) Huo, Q.; Margolese, D. I.; Ciesla, U.; Demuth, D. G.; Feng, P.; Gier, T. E.; Sieger, P.; Firouzi, A.; Chmelka, B. F.; Schuth, F.; Stucky, G. D. *Chem. Mater.* **1994**, *6*, 1176.

hexagonal phase for long-chain surfactants ($n = 20$ and 22).[40] This suggests that as the surfactant alkyl chain increases, a larger headgroup is necessary to optimize the surfactant packing parameter that affords the 2-D hexagonal phase. It can, thus, be expected that for short-chain surfactants, it may be beneficial for the formation of the 2-D hexagonal phase to decrease the effective headgroup area. Furthermore, the aforementioned example of the structure-directing behavior of C_n surfactants showed that the increase in surfactant chain length favors phases with lower surface curvature, because longer alkyl chain length resulted in the formation of a lower-surface-curvature lamellar phase. Similarly, for alkyltriethylammonium, high-surface-curvature SBA-1 phase with cage-like structure was favored for $n = 10-18$, whereas 2-D hexagonally ordered silica was obtained for $n = 20$.[7] This suggests that for a given type of surfactant, the longer the alkyl chain is, the easier it is to form a lower curvature phase, and on the contrary, the shorter the chain is, the easier it is to form a higher curvature phase. These results on the influence of headgroup size and alkyl chain length on the mesophase formation suggest that in the case of C_n surfactants, the problems with the formation of 2-D hexagonal phases for short-chain alkyls ($n < 10$) may arise from their too large effective headgroup area. This problem may be overcome using short-chain C_{n-3-n} and C_{n-n} surfactants that have smaller effective headgroup areas per single alkyl chain in the surfactant structure and, thus, may be more suitable templates for the 2-D hexagonal silicas. This contention for C_{n-3-n} is supported by the literature data indicating that in the case of $C_{16-3-16}$ surfactant, its effective headgroup area is 1.05 nm^2 (and, therefore, 0.525 nm^2 per single cetyl chain),[47] whereas C_{16} has an effective headgroup area of 0.605 nm^2.[50] Consequently, $C_{16-3-16}$ is expected to exhibit a slightly larger value of local effective surfactant packing parameter g when compared to C_{16} ($g = V/a_0l$, where V is the total volume of surfactant chains plus cosolvent molecules, if any; a_0 is the effective headgroup area, and l is the kinetic surfactant chain length), and thus, the former surfactant is expected to be more prone to form lower-surface-curvature phases. This was actually observed, because $C_{16-3-16}$ was reported to favor low-surface-curvature lamellar phase more than C_{16} did. Thus, C_{n-3-n} surfactants actually appear to exhibit slightly smaller effective headgroup sizes per alkyl chain in the surfactant structure than do C_n surfactants of the same alkyl chain length. The use of C_{n-n} surfactants provides additional opportunities, because it allows one to further reduce an effective headgroup area per surfactant alkyl chain; the headgroup area for these surfactants is not expected to be far from that of C_n surfactant, whereas C_{n-n} has two alkyl chains instead of one. Thus, using C_{n-3-n} and C_{n-n} double-chain surfactants, one can systematically decrease the headgroup size corresponding to a single alkyl chain in the surfactant structure, thus leading to surfactant packing properties favorable for formation of 2-D hexagonally ordered or disordered supramolecular-templated materials, even for extremely short surfactant chain length.

To illustrate the effects of the implementation of the two design criteria, XRD data for several silica samples synthesized using surfactants with octyl chains ($n = 8$) are shown in Figure 2. The use of double-chain C_{8-3-8} surfactant instead of using C_8 surfactant resulted in a significant increase in intensity of the XRD peak. Further optimization involving the use of C_{8-3-8} with the addition of a certain amount of C_{8-8} surfactant allowed us to obtain silica with XRD pattern exhibiting (100), (110) and (200) diffraction lines characteristic of 2-D hexagonal structure. Samples synthesized using double-chain surfactants with hexyl and heptyl chains (C6-D and C7-D) were disordered, despite the optimization of surfactants used (see Figure 1); nonetheless, the XRD patterns of these samples did exhibit clearly pronounced peaks, in contrast to featureless XRD patterns, or at best, some observable increases in intensity for products synthesized using C_n surfactants. The optimal mixtures of C_{n-3-n} and C_{n-n} gradually evolved from pure C_{n-3-n} to pure C_{n-n} as n decreased from 10 to 6. This showed that as the surfactant alkyl chain length decreases, the headgroup area per single alkyl chain needs to be lowered (as expected from the discussion presented above) by adding an increasing proportion of C_{n-n} surfactant. It should be noted that C_{n-n} with longer alkyl chain ($n = 12$, 16, 18) was found to favor low-surface-curvature lamellar phase,[7] so its ability to form supramolecular-templated materials with higher surface curvatures for a smaller n is analogous to the behavior of C_n surfactants that favor the lamellar phase for $n > 18$, as already discussed. Finally, the findings discussed above provide some insight as to why short-chain alkylamines ($C_nH_{2n+1}NH_2$) and diaminealkyls ($H_2NC_nH_{2n}NH_2$) were found suitable for the synthesis of supramolecular-templated small-pore niobium oxide[22,23] and promising for the preparation of small-pore silicas.[24] Now it is possible to relate this behavior to the small size of the primary amine headgroup and, thus, to a better ability to form inorganic−surfactant mesophase with micelles of small diameter.

The scope of the present work is distinctly different from earlier studies, wherein double chain and mixed surfactants with $n > 10$ have been successfully applied to control the structural type of silicate-surfactant composites.[7,40] The current study demonstrated that for short-chain surfactants, which are typically not suitable as supramolecular templates,[7,16] the supramolecular templating effect can be induced by the judicious choice of an appropriate double-chain surfactant or a mixture thereof, allowing for the synthesis of silicas with very small pore dimensions.

Thermogravimetry. Listed in Table 2 are thermogravimetric residues at 1270 K and weight losses between 373 and 623 K for as-synthesized samples (the weight-change curves are provided as Supporting Information). The residue can be regarded as percentage of silicon dioxide in the sample, because this temperature is high enough to ensure the essentially complete surfactant removal and a significant degree of dehydroxylation, whereas the weight loss from 373 to 623 K is expected to be close to the surfactant content.[51,52] On the basis of the above identification of weight loss events, one can conclude that the surfactant weight percent in as-synthesized material had a tendency to increase, whereas the silica content had a tendency to decrease, as the surfactant chain length increased (see Table 2). These findings are consistent with the previous reports on as-synthesized MCM-41 and MCM-48 materials synthesized using surfactants with n from 12 to 22.[16,53,54] Moreover, the surfactant weight percentages for the samples studied herein (i) did not exceed those for MCM-41 samples synthesized using longer-chain dodecyltrimethylammonium template,[16,54] (ii) were comparable to those for

(50) Stucky, G. D.; Monnier, A.; Schuth, F.; Huo, Q.; Margolese, D.; Kumar, D.; Krishnamurty, M.; Petroff, P.; Firouzi, A.; Janicke, M.; Chmelka, B. F. *Mol. Cryst. Liq. Cryst.* **1994**, *240*, 187−200.

(51) Kruk, M.; Sayari, A.; Jaroniec, M. In *Nanoporous Materials II*; Sayari, A., Jaroniec, M., Pinnavaia, T. J., Eds.; Elsevier: Amsterdam, 2000; pp 567−576.

(52) Busio, M.; Janchen, J.; van Hooff, J. M. C. *Microporous Mesoporous Mater.* **1995**, *5*, 211−218.

(53) Kruk, M.; Jaroniec, M.; Ryoo, R.; Joo, S. H. *Chem. Mater.* **2000**, *12*, 1414−1421.

(54) Jaroniec, M.; Kruk, M.; Shin, H. J.; Ryoo, R.; Sakamoto, Y.; Terasaki, O. *Microporous Mesoporous Mater.* **2001**, in press.

Table 3. Structural Properties of the Samples Determined from Nitrogen Adsorption Data

sample	BET specific surf area $m^2\ g^{-1}$	total pore vol $cm^3\ g^{-1}$	ext surf area $m^2\ g^{-1}$	primary pore vol $cm^3\ g^{-1}$	primary pore size nm
C6-D	730	0.70	110	0.29	1.96
C7-D	930	0.56	10	0.54	2.22
C8-H	850	0.54	20	0.50	2.39
C8-D	850	0.51	30	0.47	2.32
C10-H	820	0.63	70	0.51	2.61

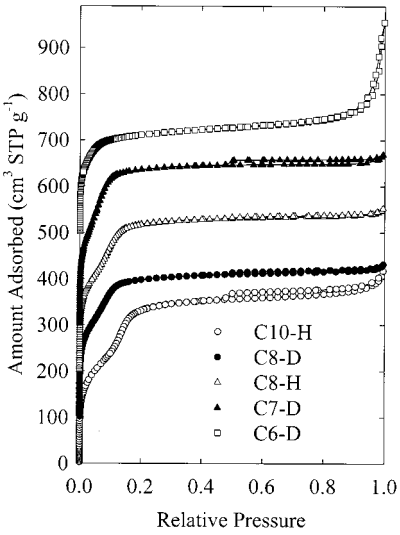

Figure 3. Nitrogen adsorption isotherms measured at 77 K for the calcined samples. Data are offset by 100, 200, 300, and 500 cm^3 STP g^{-1} for C8-D, C8-H, C7-D, and C6-D, respectively.

MCM-41 prepared using decyl- and octyltrimethylammonium surfactants, and (iii) were higher than those for amorphous and zeolitic phases obtained in the presence of hexyl-, octyl-, decyl-, and dodecyltrimethylammonium surfactants.[16] Furthermore, when one adopts the aforementioned interpretation of weight loss events and further assumes that mixed surfactants are incorporated into as-synthesized materials in the same molar ratios as those in the synthesis mixture, one can conclude that the number of moles of silica per mole of alkylammonium groups of surfactants is relatively constant and equal to about 8:1, except for C6-D material that exhibited a somewhat smaller surfactant content (see Table 2). The 8:1 ratio is similar to that for MCM-41 prepared under similar conditions using alkyltrimethylammonium or alkyltriethylammonium, or mixtures thereof with *n* from 12 to 22.[54] All of these results clearly point to the supramolecular templating's being operative in the formation of the materials under study.

Nitrogen Adsorption. Nitrogen adsorption isotherms for the calcined samples are shown in Figure 3, and the structural parameters derived from nitrogen adsorption data are listed in Table 3. In general, these isotherms exhibited an increase in the amount adsorbed up to the relative pressure somewhere between 0.06 and 0.18, depending on the particular sample, and then leveled off. Such a behavior is usually associated with adsorption in micropores, but as will be shown later, the pore size of the materials under study is close to the micropore size range, but not necessarily within this range. The C6-D sample exhibited a major increase in the amount adsorbed at pressures close to the saturation vapor pressure. This behavior is attributable to capillary condensation of nitrogen in secondary pores (interparticle voids) with some contribution of multilayer adsorption on the surface of these pores. This indicates that a considerable fraction of interparticle pores was of size below ~200−400 nm (as predicted on the basis of the Kelvin

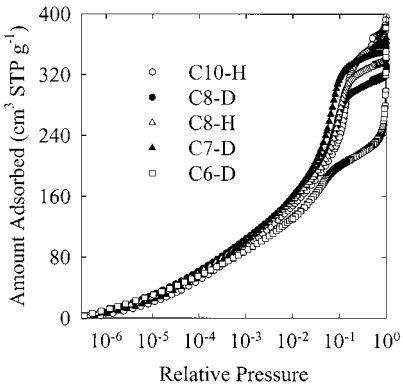

Figure 4. Nitrogen adsorption isotherms at 77 K shown in a logarithmic scale for the calcined samples.

equation[41,42,44]). For the other samples, the multilayer adsorption/capillary condensation in the interparticle pores did not provide any significant contribution to the overall adsorption, and thus, one can expect that most of these pores exhibited size above 200−400 nm. Except for C6-D, nitrogen adsorption isotherms shown in linear scale for the samples featured more or less pronounced, yet distinct condensation steps centered at relative pressures of 0.07, 0.10, 0.09, and 0.14, for C7-D, C8-H, C8-D, and C10-H, respectively (see Figure 3 and Supporting Information). In particular, the steps were clearly visible for hexagonally ordered C8-H and C10-H samples. To the best of our knowledge, these are the lowest relative pressures for which the pore filling steps were observed on nitrogen adsorption isotherms shown in linear scale (as can be seen in Figure 4, the nitrogen adsorption isotherms for all of the samples under study exhibited discernible condensation steps when shown in logarithmic scale). The previously reported relative pressures for such steps were at or above 0.15.[12,18,35] The finding that the stepwise, rather than continuous, pore filling of nitrogen at 77 K in cylindrical siliceous pores extends down to the relative pressure of 0.1 or perhaps even lower (which corresponds to the pore size of about 2.4 nm, as will be shown below) provides new insight into an important question regarding the relation between the pore size and the mechanism of gas adsorption in porous media. In the case of C6-D, the step of condensation of nitrogen in the pores was not well-pronounced, but the corresponding relative pressure can be estimated as 0.05, which is remarkably low. The adsorption isotherm for the latter material leveled off at a relative pressure of about 0.07, which indicates no broadening of the pore size distribution toward larger pore sizes. For all of the samples considered, the adsorption isotherms shown in a logarithmic scale exhibited an initial gradual increase related to the monolayer−multilayer adsorption, followed by a more steep increase attributable to the condensation of nitrogen in the primary pores (see Figure 4). Subsequently, the isotherms leveled off after the primary pores were filled with condensed adsorbate and a further increase in the amount adsorbed resulted merely from multilayer adsorption (and capillary condensation at pressures close to the saturation vapor pressure) on the external surface. This pattern of adsorption behavior clearly

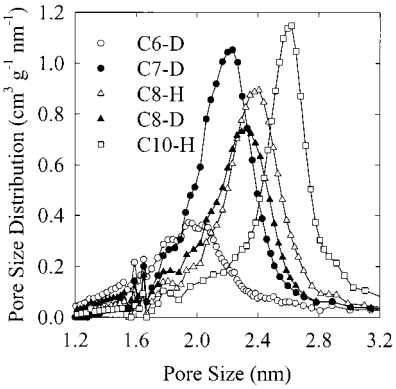

Figure 5. Pore size distributions for the calcined samples.

indicated that the pores of the samples are monodisperse and that the presence of pores considerably more narrow than the primary pores is highly unlikely.

In the case of the hexagonally ordered samples, it was possible to examine the enhancement of the low-pressure adsorption resulting from the small pore size by comparing the statistical film thickness of nitrogen adsorbed in these pores to that for MCM-41 silicas. It was found that the statistical film thickness for the small-pore samples (C8-H and C10-H) at relative pressures preceding the capillary condensation was appreciably larger than that for MCM-41 samples with larger pores (see Supporting Information); moreover, the statistical film thickness for the C8-H sample with the smallest pores among the 2-D hexagonally ordered samples considered (2.39 nm) was the highest in the entire low-pressure range. This effect can be related to the increased curvature of the surface of the relatively narrow pores, which leads to stronger adsorbate−adsorbent interactions, and to the facilitated interactions of adsorbed molecules with closely located opposite side of the pore wall and with other molecules adsorbed on it.[18]

The pore size distributions for the samples are shown in Figure 5. The PSD for C6-D was centered on the borderline between the micropore and mesopore ranges (2 nm) (see Table 3). C7-D and C8-D exhibited narrow PSD centered at about 2.2 and 2.3 nm, respectively. C8-H had a narrow PSD with a maximum at 2.39 nm, which is in excellent agreement with the pore size of 2.43 nm that was determined on the basis of geometrical considerations (eq 1). C10-H had PSD centered at 2.61 nm, which also coincided with the pore size calculated using eq 1 (2.59 nm). The pore wall thickness of these materials was calculated as a difference between the distance between the pore centers (which is equal to $2(3^{-1/2})\ d_{100}$) and the pore size calculated using eq 1. The pore wall thickness for C8-H and C10-H was 0.68 and 0.79 nm, respectively, and thus, was similar to that for typical MCM-41 silicas with larger pore sizes.[11,18] On the basis of all of the results presented above, it is clear that highly ordered MCM-41-type silicas with pore sizes as small as 2.4 and 2.6 nm were successfully synthesized. To facilitate the studies of adsorption in porous media and the development of procedures for calculation of PSDs, a nitrogen adsorption isotherm for the hexagonally ordered C8-H sample with very small pore size is reported herein in tabular form (see Supporting Information).

It should be noted that many MCM-41 silicas were claimed to exhibit similar or even lower pore sizes. However, nitrogen adsorption isotherms for most of these samples did not level off at relative pressures ≤ 0.13, as the isotherm for C8-H did, thus revealing either broader PSDs or average pore sizes above those for C8-H. Those few MCM-41-type silicas for which the reported nitrogen adsorption isotherms leveled off below the relative pressure of about 0.13[17−19,21,24,26,28] did not show distinct steps of condensation in primary pores. This may, perhaps, be related to their significantly smaller primary pore size, as in the case of samples reported in refs 24, 26, and 28, but in most cases appears to be related to a much lower degree of structural uniformity, as seen from XRD data and, thus, from considerable pore size distribution broadening. Refs 24 and 26 reported silicas with very small unit-cell sizes, whose nitrogen adsorption isotherms leveled off at very low relative pressures. One of these isotherms revealed a significant extent of the external surface of the sample, which may be related to the XRD observation that the material could contain some mesostructured impurity.[24] The second one was characteristic of a microporous material, but because low-pressure nitrogen adsorption data were not reported, it is difficult to conclude if the PSD was actually monodisperse and narrow, although this seems likely on the basis of XRD data reported. It can be concluded that the small-pore samples described herein appear to be the first well-documented, phase-pure silicas with narrow PSDs on the borderline between the micropore and mesopore size ranges. Thus, the gap between microporous and mesoporous silicas with uniform pores was finally bridged from the mesopore side.

The silicas reported herein have several attractive features as for materials with pores on the borderline between the micropore and mesopore ranges. They were stable upon calcination and exhibited narrow pore size distributions, as discussed above. In addition, their primary pore volumes and nitrogen BET specific surface areas (Table 3) were large, as for materials with so small pores. The pore volumes were not so large as for MCM-41 with larger pores, but it can be readily shown that further increase in the pore volume for hexagonally ordered silicas with small pore sizes would imply the decrease in the pore wall thickness,[55] what in turn would most likely have a detrimental effect on the structural stability. It should be noted that the values of nitrogen BET specific surface areas commonly overestimate the actual specific surface area for mesoporous silicas[56] and are inherently not reliable for microporous materials.[41] To check their reliability for the samples under study, the specific surface area was evaluated for the ordered samples as a sum of (i) the primary pore area calculated on the basis of the primary pore volume and primary pore diameter (calculated using eq 1), and (ii) the external surface area.[44] Thus, obtained geometrical specific surface areas were equal to 850 and 860 $m^2\ g^{-1}$ for C8-H and C10-H, respectively, and were in a good agreement with the nitrogen BET specific surface areas. These results suggest that nitrogen S_{BET} calculated in the relative pressure range employed is also an accurate measure of the actual specific surface area for the disordered samples under study. As can be seen in Table 3, the pore size of the samples increased as the length of the alkyl chain of the surfactants used increased. The increase corresponding to two additional carbon atoms in the alkyl chain was about 0.3 nm, which is consistent with earlier studies of MCM-41.[1,11,18,20]

Argon Adsorption. Argon adsorption isotherms measured at 77 K for the small-pore samples are shown in linear scale in Figure 6 (their parts in the capillary condensation region are shown in more detail as Supporting Information). It can be seen that the argon isotherms at 77 K were, in general, similar to nitrogen adsorption isotherms; however, in the case of C6-D, the argon adsorption did not increase to any significant extent

(55) Kruk, M.; Jaroniec, M.; Sayari, A. *Chem. Mater.* **1999**, *11*, 492−500.

(56) Kruk, M.; Antochshuk, V.; Jaroniec, M.; Sayari, A. *J. Phys. Chem. B* **1999**, *103*, 10670−10678.

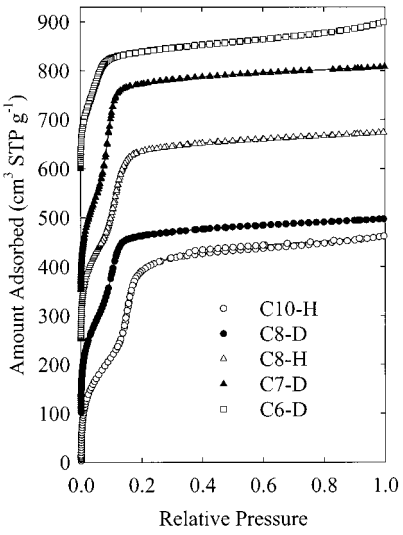

Figure 6. Argon adsorption isotherms measured at 77 K for the calcined samples. Data are offset by 100, 250, 350, and 600 cm^3 STP g^{-1} for C8-D, C8-H, C7-D, and C6-D, respectively.

in the proximity of the saturation vapor pressure, in contrast to the nitrogen adsorption behavior. This can be related to the fact that argon at 77 K does not exhibit capillary condensation in pores wider than about 20 nm,[57] this limit being apparently smaller than the size of interparticle pores of the sample. Argon adsorption isotherms at 77 K exhibited much sharper condensation steps than those on the corresponding nitrogen adsorption isotherms (compare Figures 3 and 6). This may be related to smaller statistical film thickness of argon in the pores and, thus, larger diameter of void space in the pores at the onset of condensation.[58] Similarly to the nitrogen adsorption results, the condensation step for C6-D was not distinct, being centered at a relative pressure of about 0.055, but the steps on the argon isotherms for the other samples were very clear in the linear scale. The relative pressures corresponding to the midpoints of these steps were 0.09, 0.12, 0.105, and 0.16 for C7-D, C8-H, C8-D, and C10-H, respectively. The steps on argon adsorption isotherms at 77 and 87 K have already been observed at similarly low relative pressures,[19,58] but were not so clearly pronounced. Similarly to nitrogen adsorption isotherms, low-pressure argon adsorption isotherms exhibited a gradual increase (related to monolayer−multilayer adsorption), followed by a steep rise (related to capillary condensation) and a subsequent leveling off (see Supporting Information), confirming the monodisperse nature of PSDs for the samples.

(57) Kruk, M.; Jaroniec, M., unpublished data.
(58) Kruk, M.; Jaroniec, M. *Chem. Mater.* **2000**, *12*, 222−230.

Conclusions

Hexagonally ordered and disordered silicas with narrow pore size distributions on the borderline between micropore and mesopore ranges were successfully synthesized using mixtures of *N*,*N*′-dialkyl-*N*,*N*,*N*′,*N*′-tetramethylpropane-1,3-diammonium bromides [$C_nH_{2n+1}(CH_3)_2N(CH_2)_3N(CH_3)_2C_nH_{2n+1}Br_2$] and *N*,*N*-dialkyl-*N*,*N*-dimethylammonium bromides [$(C_nH_{2n+1})_2(CH_3)_2$-NBr] as the structure-directing surfactants. The surfactants with two chains were used in order to increase the micelle-forming ability of the short alkyl (hexyl, heptyl or octyl) chains. When beneficial, these surfactants were mixed in an appropriate ratio in order to attain the packing parameter required for the formation of hexagonally ordered mesostructures. On the basis of the published XRD and adsorption data, one can conclude that the degree of ordering of the materials described herein surpasses that of the materials with pore sizes between 1.9 and 2.4 nm reported to date. The obtained materials were clearly formed via supramolecular templating, despite the use of short-chain surfactants. The structural properties, such as the surfactant content, pore wall thickness, pore volume, and specific surface area show that the obtained samples are small-pore analogues of larger-pore ordered mesoporous materials, such as MCM-41. The ordered silicas, and the 2-D hexagonally ordered ones in particular, with highly uniform pores of a size approaching the micropore range are important as model adsorbents to study fundamental aspects of adsorption in porous media. Their use allowed us to demonstrate that the two-stage pore-filling mechanism, that is, multilayer adsorption followed by condensation, persists down to the relative pressures of 0.07 or lower for nitrogen at 77 K and 0.09 or lower for argon at 77 K, which corresponds to pore sizes of 2.2 nm or lower. The reported molecular sieves with narrow pore size distributions on the borderline between the micropore and mesopore ranges are attractive for applications in separations and catalysis.

Acknowledgment. Korea Science and Engineering Foundation (project no.: 97-05-02-06-01-3) and the donors of the Petroleum Research Fund administrated by the American Chemical Society are gratefully acknowledged for their support of this research.

Supporting Information Available: Table (1) of nitrogen adsorption isotherm for C8-H silica; graphs (6) with weight change curves (1), nitrogen adsorption isotherms (1), nitrogen statistical film thickness curves (2), and argon adsorption isotherms (2). This material is available free of charge via the Internet at http://pubs.acs.org.

JA0038326